BBA - Biomembranes 1866 (2024) 184390

Contents lists available at ScienceDirect

BBA - Biomembranes

journal homepage: www.elsevier.com/locate/bbamem

The dimer of human SVCT1 is key for transport function

Menebere Woubshete [a], Lok I. Chan [a], George Diallinas [b,c], Bernadette Byrne [a,*]

[a] Department of Life Sciences, Imperial College London, London SW7 2AZ, UK
[b] Department of Biology, National and Kapodistrian University of Athens, Panepistimioupolis, 15784 Athens, Greece
[c] Institute of Molecular Biology and Biotechnology, Foundation for Research and Technology, 70013 Heraklion, Greece

ARTICLE INFO

Keywords:
Vitamin C
SVCT1
Transport
Substrate uptake
Dimerisation
Mutants

ABSTRACT

Humans and other primates lack the ability to synthesize the essential nutrient, Vitamin C, which is derived exclusively from the diet. Crucial for effective vitamin C uptake are the Na^+ dependent Vitamin C transporters, SVCT1 and SVCT2, members of the nucleobase ascorbate transporter (NAT) family. SVCT1 and 2 actively transport the reduced form of Vitamin C, ascorbic acid, into key tissues. The recent structure of the mouse SVCT1 revealed the molecular basis of substrate binding and that, like the other structurally characterised members of the NAT family, it exists as a closely associated dimer. SVCT1 is likely to function via the elevator mechanism with the core domain of each protomer able to bind substrate and move through the membrane carrying the substrate across the membrane. Here we explored the function of a range of variants of the human SVCT1, revealing a range of residues involved in substrate selection and binding, and confirming the importance of the C-terminus in membrane localisation. Furthermore, using a dominant negative mutant we show that the dimer is essential for transport function, as previously seen in the fungal homologue, UapA. In addition, we show that a localisation deficient C-terminal truncation of SVCT1 blocks correct localisation of co-expressed, associated wildtype SVCT1. These results clearly show the importance of the dimer in both correct SVCT1 trafficking and transport activity.

1. Introduction

Vitamin C is an essential nutrient with a wide range of biological functions. Vitamin C functions as a cofactor in enzymes involved in synthesis of a range of important cellular molecules including cholesterol [1] [2]. Vitamin C plays a key role in the activity of a number of hydoxylases, most famously involved in hydroxylation of proline and lysine residues, which allow correct folding of the three-dimensional structure of collagen [3]. Individuals deficient in correctly folded collagen have a reduced capacity for wound healing and an increased chance of bone fracture, both of which are characteristics of scurvy [4]. Moreover, Vitamin C has many other roles including in neurogenesis and stem cell differentiation both in developing and adult brains [5], modulation of neurotransmitter transmission in the brain [1] and regulation of gene expression via HIF hydroxylase activity [6]. A subset of Vitamin C dependent dioxygenases includes the ten-eleven translocation enzyme (TET) family and the Jumonji C domain containing histone demethylase (JHDMs) which play key roles in epigenetic regulation via DNA methylation [7]. Furthermore, Vitamin C has been demonstrated to induce opening of cystic fibrosis transmembrane conductance regulation (CFTR) Cl^- channels, thus increasing Cl^- transport [8].

As a result of its many and varied biological activities, Vitamin C also has a number of roles in human health, having protective effects against β-amyloid induced cellular stresses similar to those seen in Alzheimer's disease, in both cell and animal models [9,10], and reducing the symptoms of the common cold [11]. Vitamin C has long been thought to have anti-tumorigenic effects, initially as a result of its antioxidant effects but more recent data shows that the pro-oxidant effects of high concentrations of vitamin C can result in death of specific colorectal cancer cells [12]. Vitamin C can also be used in combination with other drugs to enhance the overall chemotherapeutic efficacy in different cancer tissues [13,14].

Most species can synthesize Vitamin C but due to the lack of a functional L-gulono-γ-lactone oxidase enzyme, key in the synthesis pathway, humans and other higher primates have to obtain their Vitamin C exclusively from their diet [15]. Given the importance of Vitamin C in health and disease, the mechanism of uptake and distribution has been the focus of much study. Vitamin C uptake is mediated by the integral membrane transport proteins, SVCT1 and SVCT2 [16], while the oxidized form of vitamin C, dehydroascorbate (DHA), is

* Corresponding author.
E-mail address: b.byrne@imperial.ac.uk (B. Byrne).

https://doi.org/10.1016/j.bbamem.2024.184390
Received 7 May 2024; Received in revised form 6 August 2024; Accepted 3 October 2024
Available online 4 October 2024

transported via glucose transporters (GLUTs). SVCT1 and 2 are members of the Nucleobase-Ascorbate transporter (NAT) family responsible for cellular uptake of metabolites in almost all species [17]. In bacteria, plants and fungi, NATs are specific for nucleobases, whereas in humans they are specific for ascorbic acid [18]. The SVCTs are sodium-dependent active transporters that couple the transport of one molecule of ascorbic acid to two sodium ions [19,20]. SVCT1 and 2 share significant sequence identity (~65 %) but differ in their function largely as a result of differential expression. SVCT1 is expressed mainly in epithelial cells of the intestine, liver and kidneys and is responsible for uptake of Vitamin C for further distribution, while SVCT2 is expressed in various tissues including epithelial cells, with particularly high levels detected in brain, eye, bone and endocrine tissues where it is likely to function to concentrate Vitamin C for use in various cellular processes [16].

The two transporters also differ in their kinetics with SVCT2 being a high-affinity/low-capacity transporter and SVCT1 a low-affinity/high-capacity transporter [19,21]. Previous work has highlighted the importance of the C-terminal region of the SVCT1 in membrane localisation [22], while differences in the sequence of the N-terminal regions of SVCT1 and SVCT2 are responsible for targeted localisation to the apical and basolateral membranes of polarized epithelial cells, respectively [23]. Other work has highlighted the importance of glycosylation for correct targeting of the SVCTs [24,25]. Like all transporters, SVCT1 is predicted to function via an alternating access mechanism where the protein alternates between outward and inward open states allowing binding of substrate from the extracellular side of the membrane and then release into the cytoplasm [26].

The structure of mouse SVCT1 (mSVCT1) was recently solved using single-particle cryogenic electron microscopy (cryo-EM) in the presence and absence of ascorbic acid [27]. The structure revealed mSVCT1's substrate binding site, identified residues important in substrate recognition and specificity, and showed the formation of an SVCT1 homodimer. It also showed close structural homology with the other structurally characterised members of the NAT family, UapA [28] and UraA [29,30]. All NAT monomers are organised into two domains; a gate or dimerisation domain and a core or transport domain. Substrate binds to the transport domain and the whole domain is thought to move through the membrane moving the substrate from one side to the other via the so-called elevator mechanism. However, a number of questions remain unanswered about the mechanism of SVCT1. Functional analysis of both UapA and UraA [28,30] reveals that the dimer is crucial for correct function of the protein, however this is yet to be characterised for SVCT1. In addition, while mutational analysis has highlighted residues key in function of the mouse SVCT1 [27], the equivalent analysis has yet to be carried out on the human protein. Here we identify human SVCT1 (hSVCT1) residues involved in substrate binding and recognition, show that the hSVCT1 dimer formation is required for transport function, and demonstrate that a C-terminally truncated variant blocks correct localisation of co-expressed wild-type (WT) hSVCT1 to the plasma membrane (PM).

2. Materials and methods

2.1. Generation of WT SVCT1 expression construct, truncated constructs and mutants

The full-length hSVCT1 gene was obtained as a synthetic gene (GeneArt). Primers for the addition of a His_8 tag and a TEV cleavage site to a pcDNA3.1-YFP vector, the amplification of full-length hSVCT1, the generation of N and C-terminal truncated and mutant variants of hSVCT1 were designed and purchased from Eurofins Genomics **(Supp Table 1)**. A pcDNA3.1-YFP-His vector was constructed by cloning in a PCR amplified fragment containing a YFP and a C-terminal His_8 tag into a pcDNA3.1 vector to produce pcDNA3.1-YFPHis_8. Full-length hSVCT1 and a range of N and C-terminal truncated variants of hSVCT1 were

Table 1
SVCT1 mutants generated and the UapA equivalents.

hSVCT1 mutant	UapA equivalent*	Location	Rationale based on UapA genetics, structure and functional assays and mSVCT1 structure
L65A	I100	TM1	Part of the extracellular substrate translocation trajectory in mSVCT1.
F112A	F155	TM3	Conserved residue of the substrate binding site in core/elevator domain. F155A substitution enlarges specificity of UapA for nucleobases.
I195A	I230	TM5	Conserved residue of scaffold domain at interface with the core/elevator domain. I230A substitution causes enhanced transport activity of UapA.
R206A	D241	TM5	Residue of the scaffold domain at interface with core/elevator domain of UapA and mSVCT1.
G387V	G411	TM10	Conserved residue in the core/elevator domain forming part of translocation channel. G411V substitution leads to loss-of-function by locking UapA in inward-facing conformation.
I439A	V463	TM12	Scaffold domain residue at interface with core/elevator domain. V463I substitution enlarges specificity for nucleobases in UapA (in the context of F528S).
L458G	R481	TM13	Scaffold domain residue located at cytoplasmic end of the substrate translocation trajectory of the associated monomer. R481G/A substitutions in UapA enlarge specificity for nucleobases and increase transport activity.
T499A	T526	TM14	Scaffold domain residue at extracellular end of substrate translocation trajectory. T526A/M substitutions in UapA enlarge specificity for nucleobases and increase transport activity.
M501A	F528	TM14	Scaffold domain residue at extracellular end of substrate translocation trajectory. F528A/S substitutions in UapA result in enlarged specificity for nucleobases and increase transport activity.
^{381}SS^{382}-^{381}TF^{382}	T405-F406	TM10	Residues of the substrate binding site in the core/elevator domain. F406A substitution in UapA results in enlarged specificity for nucleobases.
^{381}SSSP^{384}-^{381}TFAQ^{384}	^{405}TFAQ^{408}	TM10	Residues of the substrate binding site in the core/elevator domain. Mutations F406A and Q408E in UapA result in enlarged specificity for nucleobases. Mutation Q408P introducing the Pro found in SVCTs is loss-of-function in UapA.

* Based on Structure alignment (see Fig. 1b).

cloned into pcDNA3.1-YFPHis$_8$ using the In-Fusion HD Cloning kit (Takara Bio USA). This produces constructs containing hSVCT1 in frame with a C-terminal Tobacco etch virus cleavage site, YFP and a His$_8$ tag. A previous study demonstrated similar functional kinetics and localisation for eGFP and non-GFP tagged versions of hSVCT1, so we are confident that our YFP tag has little effect on transporter behaviour [31]. Mutagenesis reactions were performed using the QuikChange II Site-Directed Mutagenesis kit (Agilent). Each construct was confirmed by sequencing.

2.2. Expression of proteins

Human-derived embryonic kidney (HEK-293) cells were cultured in Dulbecco's Modified Eagle's Medium (DMEM) with 10 % foetal bovine serum (FBS) and 0.5 % Penicillin-Streptomycin in T25-cm^2 flasks. The cells were incubated at 37 °C, 5 % CO_2 and 95 % O_2, and were split every 3–4 days. Cells for transfection were plated in T25-cm^2 flasks and grown to 70–90 % confluency. These cells were transfected using 10 μg of plasmid DNA and 30 μg linear polyethylenimine MAX (Polysciences) according to the manufacturer's instructions. All downstream analyses were performed 48 h post-transfection.

2.3. Western blot analysis and in-gel fluorescence

Around 10 million transfected cells were harvested 48 h post-transfection and solubilised in 100 μl solubilisation buffer containing 50 mM Tris, pH 8.0, 150 mM NaCl, and 1 % n-dodecyl-β-D-maltoside (DDM) for 1 h at 4°C. Unbroken cells were pelleted by centrifugation at 20,000×*g* for 30 min at 4°C and cell lysates were separated on a Novex 10 % Tris-Glycine Gel (Invitrogen). In-gel fluorescence was assessed using a FLA-5000 FujiFilm imaging system and proteins were transferred onto a nitrocellulose membrane using an iBlot 2 Starter Kit (Invitrogen). The membranes were blocked in 5 % Skimmed Milk Powder in PBS with 0.2 % TWEEN-20 (PBS-T) at room temperature for 1 h and then incubated with 1:1000 diluted mouse monoclonal anti-His-Tag antibody (Dianova) at 4°C overnight. The membranes were then washed in PBS-T and subsequently incubated with 1:3000 diluted horse HRP-linked polyclonal anti-mouse IgG (Cell Signaling Technology) at room temperature for 1 h.

2.4. Localisation

Transfected cells were grown on coverslips and fixed with 4 % Paraformaldehyde (PFA) in phosphate buffered saline (PBS) for 20 min at room temperature. Cells were stained using Fluoromount-G Mounting Medium (Thermo Fisher Scientific) and visualised at 63× oil immersion objective on a Confocal 6 – Leica SP8 Inverted microscope using the 488 nm line from an Argon-Ion Laser.

2.5. Assessment of vitamin C uptake

The Ascorbic Acid Assay Kit II (Abcam) was used to measure the uptake of ascorbic acid by the different hSVCT1 constructs following the published protocol (Wang et al., 2023). In brief, 48 h post-transfection with individual hSVCT1 constructs, cells were incubated with 0.1 mM ascorbic acid for 30 min at 37 °C. After incubation, cells were harvested and homogenised in Ferric Reducing/Antioxidant and Ascorbic Acid (FRASC) lysis buffer. The lysates were added to a 96-well plate and incubated with a reaction mix, containing FRASC buffer, ascorbic acid probe and iron chloride solution, for 2–3 min. The Fe^{3+} is reduced to Fe^{2+} by the ascorbic acid present in the cells which results in a colorimetric product. The absorbance 593 nm was measured to determine the amount of ascorbic acid present in each sample. The ascorbic acid uptake was normalised relative to the expression of the specific hSVCT1, so the assay data shows how much ascorbic acid was being taken up per RFU of hSVCT1.

2.6. Xanthine uptake assay

The Xanthine/Hypoxanthine Assay Kit (Abcam) was used according to the manufacturer's instructions to measure the uptake of xanthine by several hSVCT1 constructs. WT UapA expressed in *Saccharomyces cerevisiae* FGY217 cells as previously described was used as a positive control [30,31]. 48 h post-transfection of HEK293 cells with the different SVCT1 constructs, cells were incubated with 0.4 mM xanthine for 30 min at 37 °C. UapA was transformed into the *S. cerevisiae* FGY217 strain and positive transformants were selected on URA plates. Positive transformants were grown in URA media supplemented with 2 % glucose at 30 °C with shaking, and expression of UapA was induced by addition of 2 % galactose. As for the hSVCT1 constructs, the yeast cells were incubated with 0.4 mM xanthine for 30 min at 30 °C. After incubation, cells were harvested and homogenised in assay buffer for 10 min. The lysates were added to a 96-well plate and incubated with a reaction mix, containing assay buffer, developer probe, development enzyme mix and developer solution, for 30 min. The xanthine is oxidized by the development enzyme to form an intermediate product that reacts with the developer solution/developer probe to form a colorimetric product. The absorbance at 570 nm was measured to determine the amount of xanthine present in each sample.

2.7. Statistical analysis

For the uptake assay data, significance was tested using a two-tailed unpaired *t*-test comparing the WT with other variants. All the graphs were plotted and statistical analysis carried out using GraphPad Prism 6.0.

3. Results and discussion

3.1. Mutations of hSVCT1 explored in this study

A key aim of the study was to explore precisely which residues determine the exquisite specificity of hSVCT1 for ascorbic acid. hSVCT1 is completely unable to transport nucleobases, substrates of bacterial, plant and fungal NAT proteins, as well as, rSNBT1, a close homologue of mammalian SVCTs [32]. Conversely UapA cannot transport ascorbic acid. Using a rationale based on findings from UapA genetics, UapA crystal structure and functional assays, as well as the recently published mSVCT1 structure, a range of different hSVCT1 mutants were generated (Table 1). These are described in more detail below.

Mutations in the substrate binding site (core/elevator domain). Although there is a relatively high degree of conservation in the substrate binding site of UapA and the SVCTs from both mouse and human, a number of key residues involved in substrate binding are completely different (see Fig. 1A **and** Fig. 1D). These differences concern residues in the so-called 'NAT motif' located in TM10. Whereas UapA and other nucleobase-related homologues possess the sequence TFAQ, this is replaced by SSSP in SVCTs [18,33]. Based on the above, we constructed versions of hSVCT1 with altered substrate binding sites, mirror-imaging the mutations previously made in UapA. More specifically, we constructed a double mutation replacing S381 and S382 of hSVCT1 to the equivalents of UapA, generating the double mutant ^{381}SS^{382}TF, and one quadruple substitution of all four residues, generating ^{381}SSSP^{384}TFAQ.

Mutations in the scaffold (dimerization) domain. In UapA, two residues, T526 and F528, located in TM14 in the gate (or dimerization) domain, are critical determinants of substrate specificity. Specific substitutions (e.g. T526A, T526M, F528A, F528S) allow UapA to transport, at increased rates, practically all purines and uracil [28]. We made Ala mutations of the equivalent residues in hSVCT1, T499 and M501. Residues that make up the intracellular substrate translocation cavity also

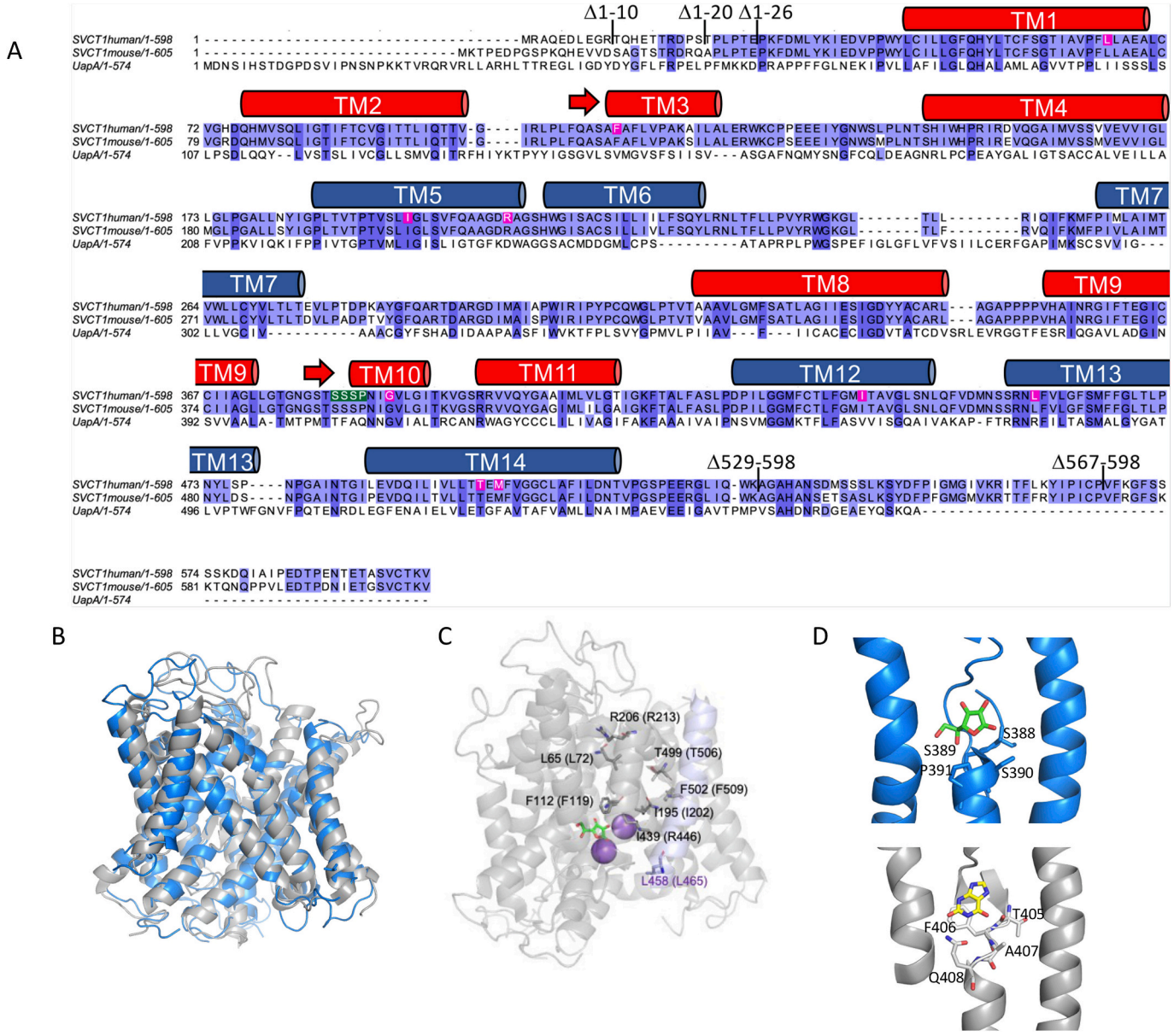

Fig. 1. Comparison of the mouse SVCT1 and UapA sequences and structures. A) Sequence alignment of SVCT1 (Human), SVCT1 (mouse) and UapA (*Aspergillus nidulans*). The residues are coloured according to sequence identity. The transmembrane (TM) domains from the mSVCT1 structure are indicated in the red and blue cylinders above the sequence. The single amino acid residues which have been substituted as part of this study are shown in pink with the binding site residues of SVCT1 highlighted in dark green. The positions of the N and C-terminal truncations are indicated by the black lines. The residues corresponding to specific TM domains are indicated by the cylinders shown above the sequence (red = core domain, blue = gate domain). B) Superposition of single protomers of mSVCT1 (blue PDB 7YTW) and UapA (grey PDB 5I6C), both in the inward facing conformation and with substrate bound (not shown for clarity). C) Structure of mSVCT1 with the amino acid residues equivalent to those playing key roles in UapA substrate selectivity indicated (hSVCT1 amino acid residue numbering shown in brackets). The mSVCT1 monomer is shown in grey, TM13 of the associated monomer is shown in light purple, the two bound Na^+ ions are shown in dark purple and ascorbic acid is shown in stick representation with green carbon atoms. D) Substrate binding sites of mouse SVCT1 (blue) and UapA (grey). The key amino acid residues involved in substrate binding are shown in stick representation and labelled with the residue number. The substrates are shown in stick representation with green (ascorbic acid) and yellow (xanthine) carbon atoms. (For interpretation of the references to colour in this figure legend, the reader is referred to the web version of this article.)

have roles in substrate specificity. Of particular interest is L458 of hSVCT1. This is the equivalent of R481 of TM13 in UapA [34], which projects into the intracellular substrate translocation channel of the opposite monomer. This appears to act as the 'final' checkpoint ensuring the transport of the correct substrate. When R481 is mutated to a Gly or Ala, UapA is able to transport practically all purines and uracil. We have generated the equivalent L458G substitution in hSVCT1. Another residue studied was I195 in TM5. This is equivalent to I230 of UapA, a conserved residue in the scaffold domain, facing the interface of the sliding elevator domain. Mutation of the equivalent residue, I230A in UapA, leads to enhanced transport activity [35].

Other mutations along the substrate translocation trajectory. It has previously been shown that the mutation G411V in UapA produced a protein that exhibits WT binding to physiological substrates (xanthine or uric acid), lacks transport activity, effectively traffics to the PM and is markedly more stable than the WT form of the protein [28,36,37]. Thus, we generated the equivalent substitution, G387V, in order to assess the effects on hSVCT1. The recently published inward-facing structure of the mSVCT1 [27] allowed identification of residues that seem to form the extracellular translocation channel, and likely guide the substrate down

to the binding site. These are residues L65, F112, R206 and I439 in hSVCT1. We generated Ala substitutions of each of these residues and analysed the corresponding mutants. Interestingly, specific mutations in residues equivalent to F112 and I439 in UapA (i.e. F155 and V463, respectively) lead to enlarged specificity (e.g. F155A) [27] or increased transport rate (V463I). [31,32]. F112/F115 forms part of the substate binding site in the core/elevator domain of hSVCT1/UapA, whereas I439/V463 is found in the scaffold domain, at the interface of the two domains.

3.2. *Effect of truncating the N- and C-terminal ends of the hSVCT1*

We assessed the expression of all the mutants and WT hSVCT1 using anti-His tag Western blot analysis (Supplementary Fig. 1). We explored the effects of a range of truncations at both the N- and C-terminal ends of hSVCT1 expressed in the HEK293 cells. All the N- and C-terminal truncations expressed to a similar level to the WT on average (Fig. 2A). All the hSVCT1 N-terminal truncations traffic effectively to the membrane, despite partial retention into cytoplasmic structures, and exhibit similar levels of activity to the WT hSVCT1 in agreement with an earlier study carried out using epithelial cells [23] (Fig. 2B and C). In contrast,

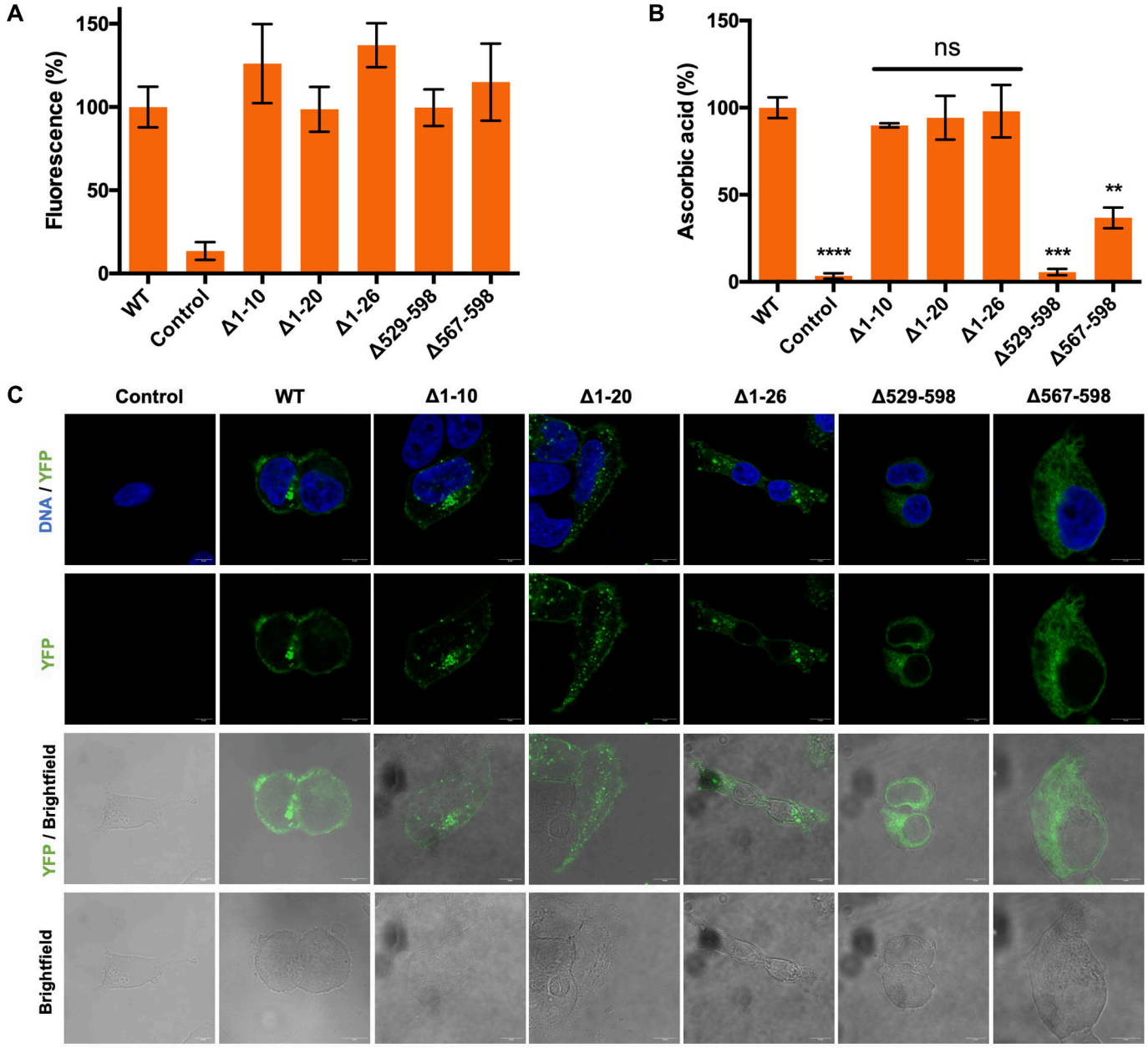

Fig. 2. Effects of N- and C-terminal truncations on expression, localisation and function of hSVCT1. **A**) Expression levels for each of the truncated forms of the protein transiently expressed as fusion proteins with a C-terminal YFP in HEK-293 cells as assessed by fluorescence measurements. The data is shown as percentage of WT hSVCT1 expression. Data is shown as an average +/− SEM ($n = 4$). Control = mock transfected cells. B) Ascorbic acid uptake activity of each of the truncated versions of hSVCT1 expressed as a percentage of WT. The raw data was first normalised to the expression levels detected in each case so that uptake amount shows the levels of ascorbic acid being taken up per RFU of hSVCT1. Data is shown as an average +/− SEM ($n = 3$). Student's *t*-test was performed between WT and truncations. ****, ***, ** = $p < 0.0001$, $p < 0.001$, $p < 0.01$ respectively. ns = not significant. C) Confocal microscopy images of cells transiently expressing WT and each of the truncated versions as indicated. The upper panel shows an overlay of YFP fluorescence and the DAPI stained nuclei, the second panel shows the YFP fluorescence only, the third panel shows an overlap of the YFP fluorescence and the brightfield image and the lower panel shows the brightfield only.

the C-terminal truncations have markedly reduced activity, with the hSVCT1Δ 529–598 construct giving similar levels of transport activity to the untransfected control and the hSVCT1△567–598 exhibiting roughly a third of the activity of WT hSVCT1 and the N-terminal truncations (Fig. 2B). This is largely due to increased levels of protein localised to the intracellular regions (Fig. 2C). As reported previously, fluorescently tagged SVCT1 that does not traffic to the membrane localises to a range of intracellular compartments [22]. Indeed, while it is clear to see that there is fluorescence visible in puncta within the cell, there is also clear fluorescence in the cytoplasm.

The results we present differ slightly from those reported for hSVCT1 stably expressed in polarized epithelial cells [22]. The Subramaniam study identified a motif ^{563}PICPVFKGFS^{572} within the C-terminal domain of hSVCT1 with a possible role in membrane localisation. Truncation of this motif from residue 566 or 562 resulted in reduced expression of hSVCT1-YFP (a very similar construct to that used in this study) and very low or no plasma membrane localisation of the protein, respectively. In contrast we see similar levels of expression, as assessed by YFP fluorescence, for the different truncated versions of the protein and although C-terminal truncation up to and including residue 567 has a significant effect on functional, membrane-localised expression in HEK293 cells, it does not completely abrogate it.

3.3. Substrate binding site mutants

We generated two binding site mutants in order to provide insights into the role of specific residues in binding and explore whether it is possible to replace the Vitamin C specific binding site of hSVCT1 with that of the xanthine/uric acid binding site of UapA. Both the double ^{381}SS^{382}TF and the quadruple mutants ^{381}SSSP^{384}TFAQ express to

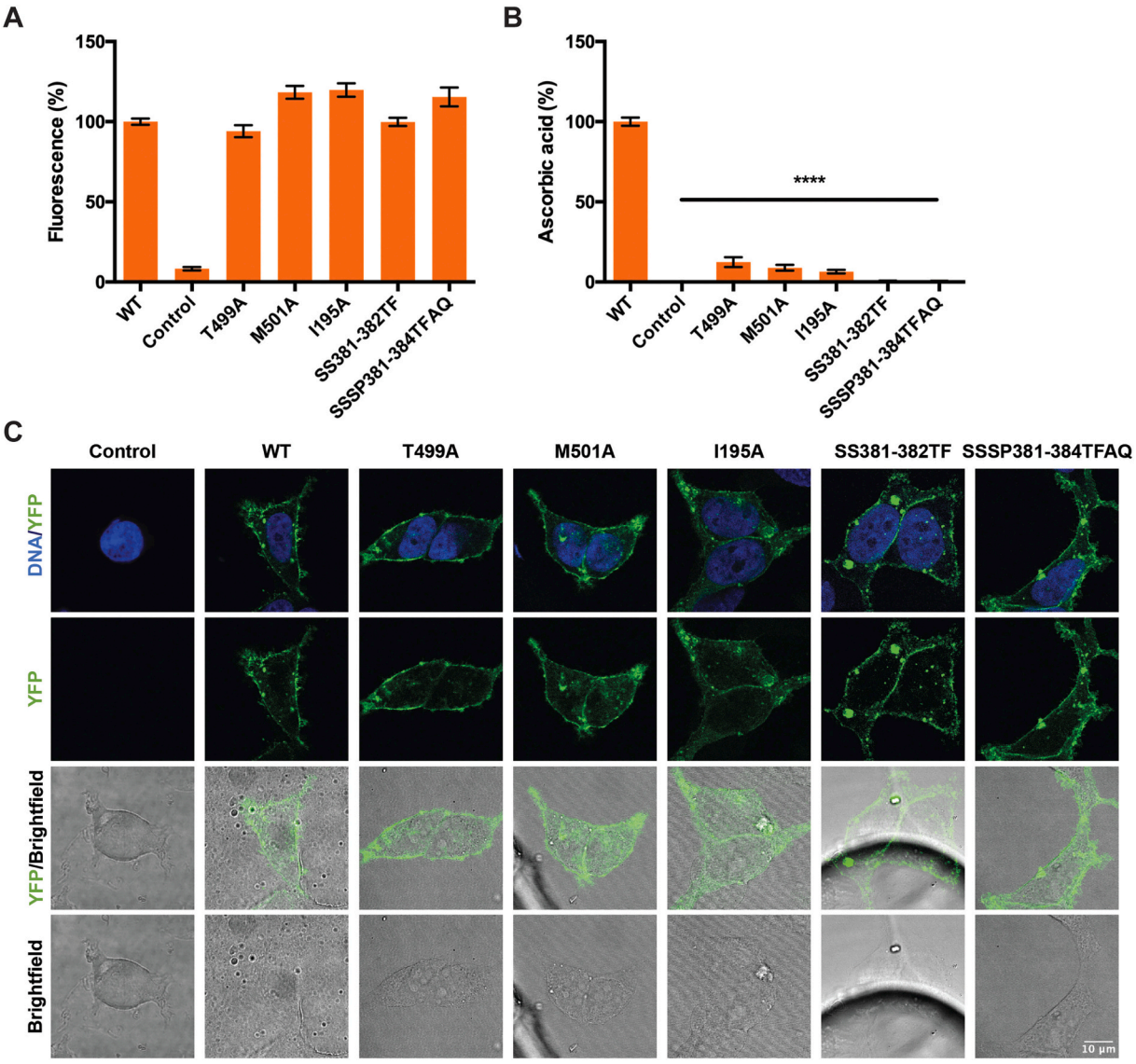

Fig. 3. Effects of substitutions at the domain interface and substrate binding site on expression, localisation and function of hSVCT1. **A**) Expression levels for each of the truncated forms of the protein transiently expressed as fusion proteins with a C-terminal YFP in HEK-293 cells as assessed by fluorescence measurements. The data is shown as percentage of WT hSVCT1 expression. Data is shown as an average +/− SEM ($n = 3$). Control = mock transfected cells. B) Ascorbic acid uptake activity of each of the mutated versions of hSVCT1 expressed as a percentage of WT. The raw data was first normalised to the expression levels detected in each case so that uptake amount shows the levels of ascorbic acid being taken up per RFU of hSVCT1. Data is shown as an average +/− SEM ($n = 4$). Student's *t*-test was performed between WT and mutants. **** = $p < 0.0001$. C) Confocal microscopy images of cells transiently expressing WT and each of the mutated versions as indicated. The upper panel shows an overlay of YFP fluorescence and the DAPI stained nuclei, the second panel shows the YFP fluorescence only, the third panel shows an overlap of the YFP fluorescence and the brightfield image and the lower panel shows the brightfield only.

similar levels as the WT protein and are plasma membrane localised, however, result in a complete loss of ascorbic acid uptake indicating that just two substitutions at the binding site are sufficient to prevent any ascorbic acid transport (Fig. 3). Despite recapitulating the UapA binding site, the ^{381}SSSP^{384}TFAQ is not able to transport xanthine either alone or in combination with L458G (equivalent to R481G in UapA) and L458G + T499A (equivalent to T526A of UapA) (Supplementary Fig. 2). Both these mutants increase transporter activity and substrate specificity in UapA. These findings indicate that there is much more to substrate selectivity in hSVCT1 than just interaction with key residues in the binding site and that there are some subtle but key differences between the mechanisms of UapA and hSVCT1.

3.4. Domain interface residues

hSVCT1-T499 and hSVCT1-M501 of TM14 are equivalent to T526 and F528 of UapA respectively (Fig. 1). Positioned at the interface between the gate and core domains, these two residues are close to but play no role in the substrate binding site. The T526A/M/S and F528S substitutions contribute to an expanded substrate profile, particularly in

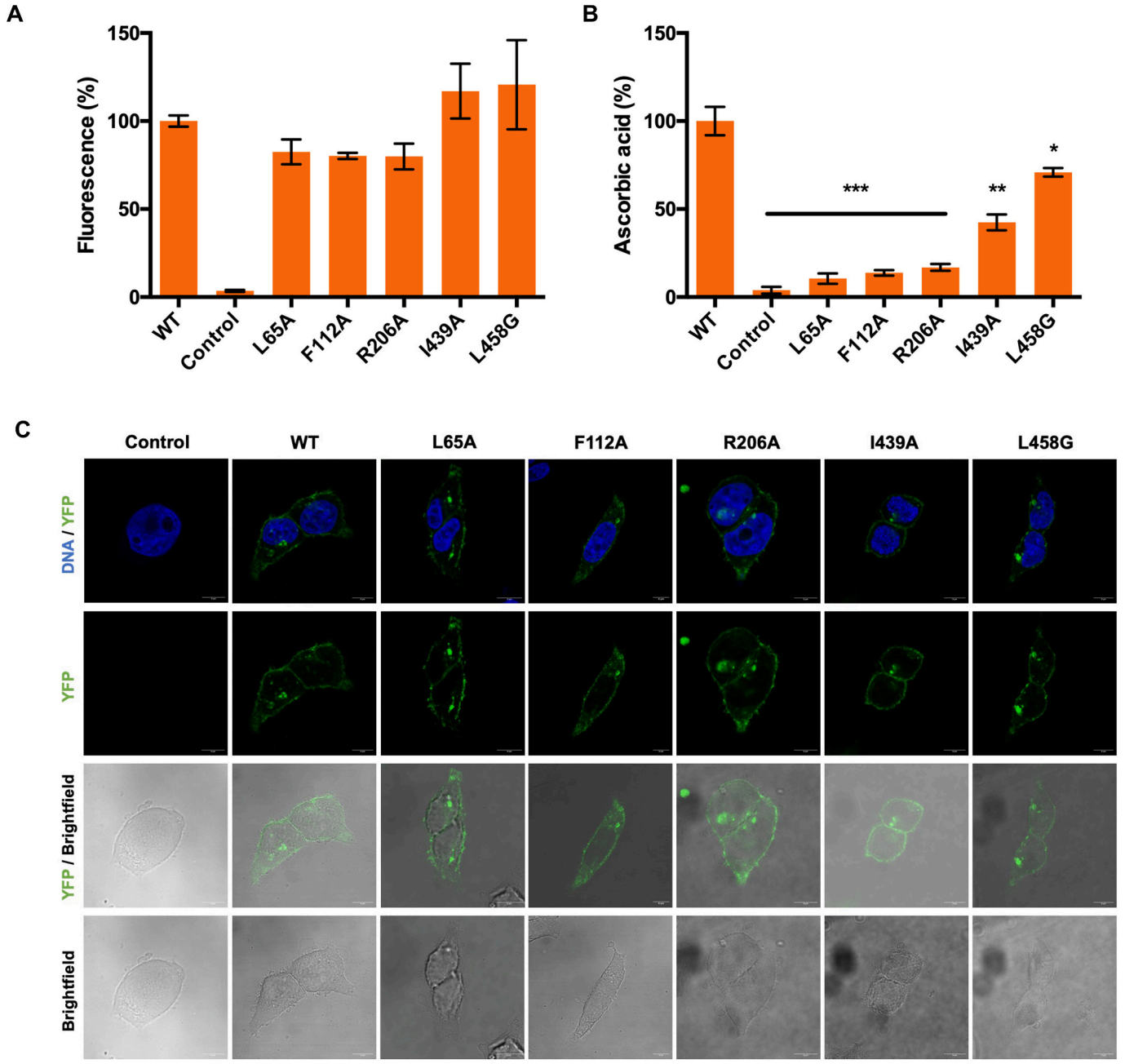

Fig. 4. Effects of substitutions in the translocation channel on expression, localisation and function of hSVCT1. A) Expression levels for each of the truncated forms of the protein transiently expressed as fusion proteins with a C-terminal YFP in HEK-293 cells as assessed by fluoresence measurements. The data is shown as percentage of WT hSVCT1 expression. Data is shown as an average +/− SEM ($n = 3$). Control = mock transfected cells. B) Ascorbic acid uptake activity of each of the mutated versions of hSVCT1 expressed as a percentage of WT. The raw data was first normalised to the expression levels detected in each case so that uptake amount shows the levels of ascorbic acid being taken up per RFU of hSVCT1. Data is shown as an average +/− SEM (n = 3). Student's *t*-test was performed between WT and mutants. ***, **, * = $p < 0.001$, $p < 0.01$, $p < 0.05$. C) Confocal microscopy images of cells transiently expressing WT and each of the mutated versions as indicated. The upper panel shows an overlay of YFP fluorescence and the DAPI stained nuclei, the second panel shows the YFP fluorescence only, the third panel shows an overlay of the YFP fluorescence and the brightfield image and the lower panel shows the brightfield only.

combination with other mutations but importantly they have little or no effect on xanthine and uric acid uptake [28]. Interestingly the T499A and M501A mutations have profound effects on the ascorbic acid uptake ability of hSVCT1 (Fig. 3) although they both express and localise similar to WT hSVCT1. It remains unclear what precise role these residues are playing. Given their location at the domain interface, it is possible that they are involved in the conformational rearrangements associated with the transport cycle. Currently there are only inward state structures of mSVCT1 [27] and other NAT proteins. An outward facing structure of one or more of these might shed light on the role of these residues as well as insights into the differences between the NAT family members.

3.5. Translocation channel mutants

Individual alanine substitutions of the residues lining the extracellular translocation channel (L65A, F112, R206 and I439) of hSVCT1 were generated. All of these caused a substantial reduction on the uptake of ascorbic acid of between 40 and 90 % although had similar expression levels and localisation to the WT transporter. This is in broad agreement with the equivalent mutations made in mSVCT1 [27]. The L458 residue of hSVCT1 is equivalent to R481 of UapA (Fig. 1A). This forms part of the intracellular translocation channel of the associated monomer, with the substrate passing this residue just before it exits the protein and released into the cytoplasm. The R481G mutation of UapA results in a transporter that has slightly reduced xanthine and uric acid uptake activity but also has limited capacity to also uptake other non-native substrates, hypoxanthine and adenine, an ability that is enhanced in combination with other substrate specificity mutants [28]. The hSVCT1-L458G substitution expresses similar to WT (Fig. 4A and C) but has significantly reduced ability to uptake ascorbic acid (Fig. 4**B**). This substitution both alone and in combination with other mutations does not confer the ability to uptake xanthine (Supplementary Fig. 2).

3.6. Functional role of dimerisation of SVCT1

SVCT1, like the bacterial and fungal homologues UraA and UapA is a dimer. In each case, the dimer interface is formed exclusively by the gate or dimerisation domain [27,28,30]. Previous analysis has shown that dimerisation of UapA is key for effective transit from the endoplasmic reticulum [38] and function [28,39] and plays a role in substrate selectivity [28]. It is not clear if individual protomers of hSVCT1 affect the activity of the associated protomer. We are able to transfect double the amount of WT hSVCT1 encoding vector DNA and obtain roughly double the amount of protein expression as assessed by fluoresence (Fig. 5A) and ascorbic acid uptake activity (~200 %) compared to when we transfect the normal amount of DNA, indicating that twice as much active transport protein is expressed and translocated to the PM (Fig. 5B). In contrast, the hSVCT1-G387V mutant, although trafficking effectively to the membrane exhibits no ascorbic acid uptake (Fig. 5B and D), although it expresses to similar levels as the WT (Fig. 5A). Analogous to the equivalent mutant in UapA G411V, it is likely that this is due to the additional bulk of the Val side chain inhibiting movement of the core, or substrate binding domain key for transport via the elevator mechanism [28]. Co-transfection of WT hSVCT1 DNA with the DNA encoding the non-functional hSVCT1-G387V results in four different forms of the dimer (WT/WT, WT/G387V, G387V/WT and G387V/G387V) (Fig. 5C). If there is no crosstalk between the individual protomers in the dimer, with each monomer working independently then there should be roughly 100 % activity overall, equivalent to the single amount of WT DNA. However, we see only ~50 % activity indicating that only the WT/WT form of the protein is transport active and the WT/G387V and G387V/WT forms of the protein in addition to the G387V/G387V are inactive. These results strongly indicate that there is functional crosstalk between the monomers in the dimer. Similar results were obtained when WT hSVCT was co-expressed with hSVCT1Δ529–598, which does not correctly localise to the plasma membrane (Fig. 5B and D) but when co-transfected with WT expresses to similar levels as the WT/WT (Fig. 5A). This suggests that both protomers of the dimer have to contain the appropriate targeting signals to allow correct localisation, perhaps required as a quality control. In other words, the G387V mutant and the Δ529–598 are dominant negative forms blocking activity or correct membrane trafficking of any associated WT monomers.

4. Conclusion

Our analysis has highlighted a number of amino acid residues of hSVCT1 involved in either substrate selection or binding. hSVCT1 seems to be more sensitive to changes than UapA, with virtually every single substitution resulting in low or no ascorbic acid uptake. This includes those residues, T499A and M501A, that are not in either the binding site or the translocation channel. In contrast, the equivalent substitutions in UapA have little effect on native substrate transport but support transport of additional non-native substrates [28]. These findings suggest that there are subtle differences in the mechanism of action of the two proteins even if they share a very similar structural architecture.

Changing residues in the substrate binding site has profound effects in both proteins (TFAQ in UapA and SSSP in hSVCT1). Previously specific substitutions of the Phe406 or Gln408 residues in UapA (eg F406A or Q408E) have been shown to affect substrate binding and transport [33,34,36,40], while introducing the residues found in SVCTs (e.g Q408P or ^{405}TFAQ^{408} ^{405}SSSP^{408}) has led to mostly loss-of-function in respect to nucleobase transport [41]. Thus, engineering ascorbic acid transport capacity in UapA is feasible by simply introducing residues that mimic the presumed binding site of SVCT1/2. Here substituting the SSSP of the hSVCT1 for the TFAQ of UapA also results in a complete loss of ascorbic acid uptake with no measurable xanthine uptake. This is also true when combining the TFAQ substitution with T499A and L458G, suggesting selection and binding specificity for ascorbic acid is multifaceted, involving several regions of the protein. Overall, it seems that a deeper analysis of co-evolving aminoacid combinations in specific transporters is required to engineer more radical specificity modifications in the NAT family.

Use of a dominant negative mutant has allowed us to clearly demonstrate that the hSVCT1 dimer is the functional form of the protein, with each protomer in the dimer influencing the activity of the associated molecule as we have reported previously for UapA [28] and others have reported for UraA [30]. Importantly both protomers also have to be competent for trafficking to the PM for the dimer to be correctly localised. It is possible that quality control checks only allow the dimer protein to go to the membrane when both C-terminal localisation motifs are present and properly folded.

Still many questions about the mechanisms of hSVCT1 remain including precisely what conformational changes are required for the protein to rearrange into the outward facing state, how lipids influence the activity of the protein and precisely what structural determinants allow the selection, binding and transport of ascorbic acid. Additional structures should help to answer some of these questions.

CRediT authorship contribution statement

Menebere Woubshete: Writing – review & editing, Visualization, Validation, Investigation, Formal analysis, Conceptualization. **Lok I. Chan:** Writing – review & editing, Visualization, Methodology, Formal analysis, Data curation. **George Diallinas:** Writing – review & editing, Formal analysis, Conceptualization. **Bernadette Byrne:** Writing – original draft, Supervision, Project administration, Funding acquisition, Conceptualization.

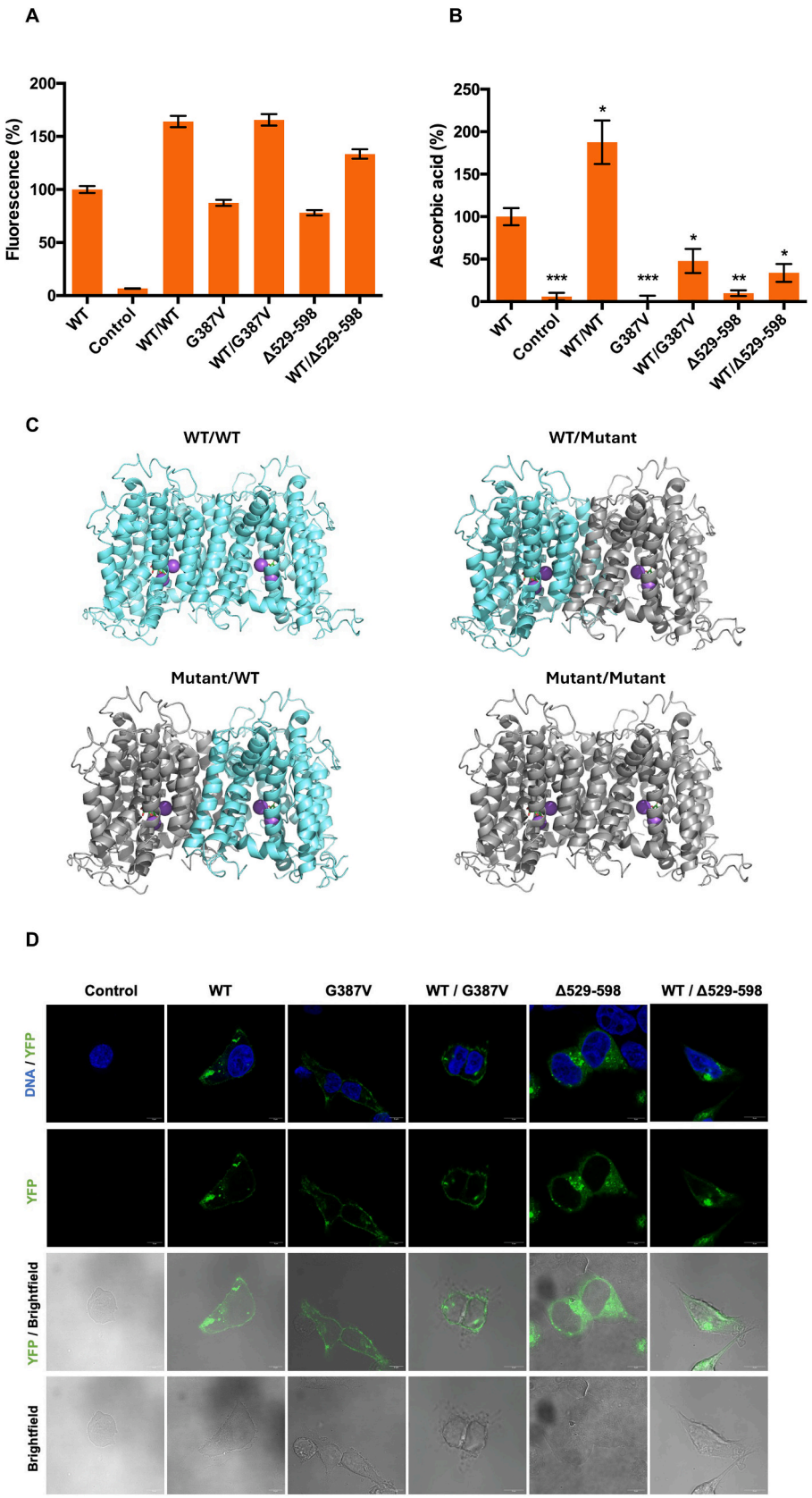

(caption on next page)

Fig. 5. Effect of co-expression of WT and dominant negative variants on function and localisation of hSVCT1. A) Expression levels for the different hSVCT1 constructs expressed either alone or in combination, as fusion proteins with a C-terminal YFP in HEK-293 cells as assessed by fluoresence measurements. B) Ascorbic acid uptake activity of different forms of hSVCT1 expressed as a percentage of WT transfected as a single dose of DNA (WT). The raw data was first normalised to the expression levels detected in each case so that uptake amount shows the levels of ascorbic acid being taken up per RFU of hSVCT1. Transfecting twice the amount of WT DNA (WT/WT) results in roughly twice the amount of ascorbic acid uptake activity. Data is shown as an average +/− SEM ($n = 3$). Student's *t*-test was performed between WT and mutants/dimers. ***, **, * = $p < 0.001$, $p < 0.01$, $p < 0.05$. C) Schematic showing the different forms of the hSVCT1 which form when WT is co-expressed with the G387V mutant. WT protein is shown in cyan and the G387V mutant in grey. The substrate is shown in stick representation with green coloured carbon atoms and the Na + ions are shown as purple spheres. D) Confocal microscopy images of cells transiently expressing WT and mutated/truncated versions alone and in combination as indicated. The upper panel shows an overlay of YFP fluorescence and the DAPI stained nuclei, the second panel shows the YFP fluorescence only, the third panel shows an overlap of the YFP fluorescence and the brightfield image and the lower panel shows the brightfield only. (For interpretation of the references to colour in this figure legend, the reader is referred to the web version of this article.)

Declaration of competing interest

The authors declare that they have no known competing financial interests or personal relationships that could have appeared to influence the work reported in this paper.

Acknowledgments

MW is funded by an Imperial College London, Department of Life Sciences PhD studentship. This research was supported by BBSRC grant BB/V006487/2 awarded to BB.

Appendix A. Supplementary data

Supplementary data to this article can be found online at https://doi.org/10.1016/j.bbamem.2024.184390.

References

[1] F.E. Harrison, J.M. May, Vitamin C function in the brain: vital role of the ascorbate transporter SVCT2, Free Radic. Biol. Med. 46 (2009) 719–730, https://doi.org/10.1016/j.freeradbiomed.2008.12.018.
[2] S. Englard, S. Seifter, The biochemical functions of ascorbic acid, Annu. Rev. Nutr. 6 (1986) 365–406, https://doi.org/10.1146/annurev.nu.06.070186.002053.
[3] E. Ramírez, N. Jara, L. Ferrada, K. Salazar, F. Martínez, M.J. Oviedo, J. Tereszczuk, S. Ramírez-Carbonell, A. Vollmann-Zwerenz, P. Hau, F. Nualart, Glioblastoma invasiveness and collagen secretion are enhanced by vitamin C, Antioxid. Redox Signal. 37 (2022) 538–559, https://doi.org/10.1089/ars.2021.0089.
[4] A.W. Ham, H.C. Elliott, The bone and cartilage lesions of protracted moderate scurvy, Am. J. Pathol. 14 (1938) 323-336.5.
[5] K. Salazar, N. Jara, E. Ramírez, I. de Lima, J. Smith-Ghigliotto, V. Muñoz, L. Ferrada, F. Nualart, Role of vitamin C and SVCT2 in neurogenesis, Front. Neurosci. 17 (2023) 1155758, https://doi.org/10.3389/fnins.2023.1155758.
[6] W.G. Kaelin, P.J. Ratcliffe, Oxygen sensing by metazoans: the central role of the HIF hydroxylase pathway, Mol. Cell 30 (2008) 393–402, https://doi.org/10.1016/j.molcel.2008.04.009.
[7] J.I. Young, S. Züchner, G. Wang, Regulation of the epigenome by vitamin C, Annu. Rev. Nutr. 35 (2014) 1–20, https://doi.org/10.1146/annurev-nutr-071714-034228.
[8] H. Fischer, C. Schwarzer, B. Illek, Vitamin C controls the cystic fibrosis transmembrane conductance regulator chloride channel, P Natl Acad Sci Usa 101 (2004) 3691–3696, https://doi.org/10.1073/pnas.0308393100.
[9] S. Rosales-Corral, D. Tan, R.J. Reiter, M. Valdivia-Velázquez, G. Martínez-Barboza, J.P. Acosta-Martínez, G.G. Ortiz, Orally administered melatonin reduces oxidative stress and proinflammatory cytokines induced by amyloid-β peptide in rat brain: a comparative, in vivo study versus vitamin C and E, J. Pineal Res. 35 (2003) 80–84, https://doi.org/10.1034/j.1600-079x.2003.00057.x.
[10] J. Huang, J.M. May, Ascorbic acid protects SH-SY5Y neuroblastoma cells from apoptosis and death induced by β-amyloid, Brain Res. 1097 (2006) 52–58, https://doi.org/10.1016/j.brainres.2006.04.047.
[11] H. Hemilä, E. Chalker, Vitamin C reduces the severity of common colds: a meta-analysis, BMC Public Health 23 (2023) 2468, https://doi.org/10.1186/s12889-023-17229-8.
[12] J. Yun, E. Mullarky, C. Lu, K.N. Bosch, A. Kavalier, K. Rivera, J. Roper, I.I.C. Chio, E.G. Giannopoulou, C. Rago, A. Muley, J.M. Asara, J. Paik, O. Elemento, Z. Chen, D.J. Pappin, L.E. Dow, N. Papadopoulos, S.S. Gross, L.C. Cantley, Vitamin C selectively kills KRAS and BRAF mutant colorectal cancer cells by targeting GAPDH, Science 350 (2015) 1391–1396, https://doi.org/10.1126/science.aaa5004.
[13] J. Qiu, T. Yang, Y. Long, P. He, W. Shen, B. Zhang, X. Shi, L. Peng, Z. Li, X. Zhang, Mitochondrial respiration inhibitor enhances the anti-tumor effect of high-dose ascorbic acid in castration-resistant prostate cancer, J. Mol. Med. 101 (2023) 125–138, https://doi.org/10.1007/s00109-022-02273-5.
[14] Y. Ma, J. Chapman, M. Levine, K. Polireddy, J. Drisko, Q. Chen, High-dose parenteral ascorbate enhanced Chemosensitivity of ovarian Cancer and reduced toxicity of chemotherapy, Sci. Transl. Med. 6 (2014) 222ra18, https://doi.org/10.1126/scitranslmed.3007154.
[15] J. Fujii, Ascorbate is a multifunctional micronutrient whose synthesis is lacking in primates, J. Clin. Biochem. Nutr. 69 (2021) 1–15, https://doi.org/10.3164/jcbn.20-181.
[16] H. Tsukaguchi, T. Tokui, B. Mackenzie, U.V. Berger, X.Z. Chen, Y. Wang, R. F. Brubaker, M.A. Hediger, A family of mammalian Na+−dependent L-ascorbic acid transporters, Nature 399 (1999) 70–75, https://doi.org/10.1038/19986.
[17] C. Gournas, I. Papageorgiou, G. Diallinas, The nucleobase-ascorbate transporter (NAT) family: genomics, evolution, structure-function relationships and physiological role, Mol. BioSyst. 4 (2008) 404–416, https://doi.org/10.1039/b719777b.
[18] A. Kourkoulou, A.A. Pittis, G. Diallinas, Evolution of substrate specificity in the nucleobase-ascorbate transporter (NAT) protein family, microb, Cell 5 (2018) 280–292, https://doi.org/10.15698/mic2018.06.636.
[19] A. Godoy, V. Ormazabal, G. Moraga-Cid, F.A. Zúñiga, P. Sotomayor, V. Barra, O. Vasquez, V. Montecinos, L. Mardones, C. Guzmán, M. Villagrán, L.G. Aguayo, S. A. Oñate, A.M. Reyes, J.G. Cárcamo, C.I. Rivas, J.C. Vera, Mechanistic insights and functional determinants of the transport cycle of the ascorbic acid transporter SVCT2 ACTIVATION BY SODIUM AND ABSOLUTE DEPENDENCE ON BIVALENT CATIONS*, J. Biol. Chem. 282 (2007) 615–624, https://doi.org/10.1074/jbc.m608300200.
[20] H. Wang, B. Dutta, W. Huang, L.D. Devoe, F.H. Leibach, V. Ganapathy, P.D. Prasad, Human Na+−dependent vitamin C transporter 1 (hSVCT1): primary structure, functional characteristics and evidence for a non-functional splice variant, Biochim. Biophys. Acta Biomembr. 1461 (1999) 1–9, https://doi.org/10.1016/s0005-2736(99)00182-0.
[21] I. Savini, A. Rossi, C. Pierro, L. Avigliano, M.V. Catani, SVCT1 and SVCT2: key proteins for vitamin C uptake, Amino Acids 34 (2007) 347–355, https://doi.org/10.1016/j.bbaexp.2005.11.002.
[22] V.S. Subramanian, J.S. Marchant, M.J. Boulware, H.M. Said, A C-terminal region dictates the apical plasma membrane targeting of the human sodium-dependent vitamin C transporter-1 in polarized epithelia, J. Biol. Chem. 279 (2004) 27719–27728, https://doi.org/10.1074/jbc.m400876200.
[23] S. Varma, K. Sobey, C.E. Campbell, S.-M. Kuo, Hierarchal contribution of N- and C-terminal sequences to the differential localization of homologous sodium-dependent vitamin C transporters, SVCT1 and SVCT2, Epithelial Cells, Biochemistry-Us 48 (2009) 2969–2980, https://doi.org/10.1021/bi802294v.
[24] A.M. Velho, S.M. Jarvis, Topological studies of hSVCT1, the human sodium-dependent vitamin C transporter and the influence of N-glycosylation on its intracellular targeting, Exp. Cell Res. 315 (2009) 2312–2321, https://doi.org/10.1016/j.yexcr.2009.04.007.
[25] V.S. Subramanian, J.S. Marchant, J.C. Reidling, H.M. Said, N-glycosylation is required for Na+−dependent vitamin C transporter functionality, Biochem Bioph Res Co 374 (2008) 123–127, https://doi.org/10.1016/j.bbrc.2008.06.120.
[26] O. Jardetzky, Simple allosteric model for membrane pumps, Nature 211 (1966) 969–970, https://doi.org/10.1038/211969a0.
[27] M. Wang, J. He, S. Li, Q. Cai, K. Zhang, J. She, Structural basis of vitamin C recognition and transport by mammalian SVCT1 transporter, Nat. Commun. 14 (2023) 1361, https://doi.org/10.1038/s41467-023-37037-3.
[28] Y. Alguel, S. Amillis, J. Leung, G. Lambrinidis, S. Capaldi, N.J. Scull, G. Craven, S. Iwata, A. Armstrong, E. Mikros, G. Diallinas, A.D. Cameron, B. Byrne, Structure of eukaryotic purine/H(+) symporter UapA suggests a role for homodimerization in transport activity., nature, Communications 7 (2016) 11336, https://doi.org/10.1038/ncomms11336.
[29] F. Lu, S. Li, Y. Jiang, J. Jiang, H. Fan, G. Lu, D. Deng, S. Dang, X. Zhang, J. Wang, N. Yan, Structure and mechanism of the uracil transporter UraA, Nature 472 (2011) 243–246, https://doi.org/10.1038/nature09885.
[30] X. Yu, G. Yang, C. Yan, J.L. Baylon, J. Jiang, H. Fan, G. Lu, K. Hasegawa, H. Okumura, T. Wang, E. Tajkhorshid, S. Li, N. Yan, Dimeric structure of the uracil: proton symporter UraA provides mechanistic insights into the SLC4/23/26 transporters, Cell Res. 27 (2017) 1020–1033, https://doi.org/10.1038/cr.2017.83.
[31] J.C. Boyer, C.E. Campbell, W.J. Sigurdson, S.-M. Kuo, Polarized localization of vitamin C transporters, SVCT1 and SVCT2, in epithelial cells, Biochem. Biophys. Res. Commun. 334 (2005) 150–156, https://doi.org/10.1016/j.bbrc.2005.06.069.
[32] S. Yamamoto, S. Yamamoto, K. Inoue, K. Inoue, T. Murata, T. Murata, S. Kamigaso, S. Kamigaso, T. Yasujima, T. Yasujima, J. Maeda, J. Maeda, Y. Yoshida, Y. Yoshida, K. Ohta, K. Ohta, H. Yuasa, H. Yuasa, Identification and functional characterization of the first nucleobase transporter in mammals: implication in the species difference in the intestinal absorption mechanism of nucleobases and their analogs

between higher primates and other mammals, J. Biol. Chem. 285 (2010) 6522–6531, https://doi.org/10.1074/jbc.m109.032961.
[33] A. Kourkoulou, I. Zantza, K. Foti, E. Mikros, G. Diallinas, Context-dependent cryptic roles of specific residues in substrate selectivity of the UapA purine transporter, J. Mol. Biol. 433 (2021) 166814, https://doi.org/10.1016/j.jmb.2021.166814.
[34] V. Kosti, I. Papageorgiou, G. Diallinas, Dynamic elements at both Cytoplasmically and extracellularly facing sides of the UapA transporter selectively control the accessibility of substrates to their translocation pathway, J. Mol. Biol. 397 (2010) 1132–1143, https://doi.org/10.1016/j.jmb.2010.02.037.
[35] D. Dimakis, Y. Pyrris, G. Diallinas, Transmembrane helices 5 and 12 control transport dynamics, substrate affinity, and specificity in the elevator-type UapA transporter, Genetics 222 (2022) iyac107, https://doi.org/10.1093/genetics/iyac107.
[36] M. Koukaki, A. Vlanti, S. Goudela, A. Pantazopoulou, H. Gioule, S. Tournaviti, G. Diallinas, The nucleobase-ascorbate transporter (NAT) signature motif in UapA defines the function of the purine translocation pathway, J. Mol. Biol. 350 (2005) 499–513, https://doi.org/10.1016/j.jmb.2005.04.076.
[37] J. Leung, A.D. Cameron, G. Diallinas, B. Byrne, Stabilizing the heterologously expressed uric acid-xanthine transporter UapA from the lower eukaryote aspergillus nidulans, Mol. Membr. Biol. 30 (2013) 32–42, https://doi.org/10.3109/09687688.2012.690572.
[38] O. Martzoukou, M. Karachaliou, V. Yalelis, J. Leung, B. Byrne, S. Amillis, G. Diallinas, Oligomerization of the UapA purine transporter is critical for ER-exit, plasma membrane localization and turnover, J. Mol. Biol. 427 (2015) 2679–2696, https://doi.org/10.1016/j.jmb.2015.05.021.
[39] E. Pyle, A.C. Kalli, S. Amillis, Z. Hall, A.M. Lau, A.C. Hanyaloglu, G. Diallinas, B. Byrne, A. Politis, Structural lipids enable the formation of functional oligomers of the eukaryotic purine symporter UapA, cell, Chem. Biol. 25 (2018) 840–848.e4, https://doi.org/10.1016/j.chembiol.2018.03.011.
[40] I. Papageorgiou, C. Gournas, A. Vlanti, S. Amillis, A. Pantazopoulou, G. Diallinas, Specific interdomain synergy in the UapA transporter determines its unique specificity for uric acid among NAT carriers, J. Mol. Biol. 382 (2008) 1121–1135, https://doi.org/10.1016/j.jmb.2008.08.005.
[41] A. Kourkoulou, P. Grevias, G. Lambrinidis, E. Pyle, M. Dionysopoulou, A. Politis, E. Mikros, B. Byrne, G. Diallinas, Specific residues in a purine transporter are critical for dimerization, ER exit, and function, Genetics 213 (2019) 1357–1372, https://doi.org/10.1534/genetics.119.302566.